X-ray structural studies of the entire extra-cellular region of the Ser/Thr kinase PrkC from Staphylococcus aureus

Alessia Ruggiero, Flavia Squeglia, Daniela Marasco, Roberta Marchetti, Antonio Molinaro, Rita Berisio

X-ray structural studies of the entire extra-cellular region of the Ser/Thr kinase PrkC from *Staphylococcus aureus*

Alessia Ruggiero[1§], Flavia Squeglia[1,2§], Daniela Marasco[1,2], Roberta Marchetti[2], Antonio Molinaro[2], Rita Berisio[1]

[1]Institute of Biostructures and Bioimaging, CNR, Via Mezzocannone 16. I-80134 – Napoli, Italy,

[2]University of Naples "Federico II", I-80134 – Via Cinthia 4, I-80126 - Napoli, Italy,

Correspondence to: Rita Berisio, Tel: 00390812534507, Fax: 00390812536642,

E-mail: rita.berisio@unina.it

[§] These authors equally contributed to this work.

Running title: *Structure of the extracellular region of PrkC*

SUMMARY

Bacterial Ser/Thr kinases modulate a wide number of cellular processes. PrkC kinase from human pathogen *Staphylococcus aureus* was also shown to induce germination of *Bacillus subtilis* spores, in response to cell-wall muropeptides. The presence of muropeptides in the bacterial extra-cellular milieu is a strong signal that growing conditions are promising. We report here the x-ray structure of the entire extra-cellular region of PrkC from *Staphylococcus aureus*. This structure reveals that the extra-cellular region of PrkC, EC-PrkC, is a linear modular structure, composed of three PASTA domains and an unpredicted C-terminal domain, which presents the typical features of adhesive proteins. Using several solution techniques, we also evidenced that EC-PrkC shows no tendency to dimerise even in the presence of high concentrations of muropeptides. X-ray structural results obtained here provide molecular clues into the mechanism of muropeptide-induced PrkC activation.

Keywords: *cell wall, crystal structure, peptidoglycan*

INTRODUCTION

Signal transduction through reversible protein phosphorylation is a key regulatory mechanism of both prokaryotes and eukaryotes. Phosphorylation frequently occurs in response to environmental signals and is mediated by specific protein kinases. Generally, phosphorylation is coupled to dephosphorylation reactions catalysed by protein phosphatases.
Eukaryotic-type serine/threonine kinases are expressed in many prokaryotes including a broad range of pathogens. The first reported eukaryotic-type serine/threonine kinase, Pkn1 from *Myxococcus xanthus*, was found to be required for normal bacterial development [1]. The advance of genome sequencing has prompted the identification of similar kinases in many bacteria. These kinases are now known to regulate various cellular functions, such as biofilm formation [2], cell wall biosynthesis [3, 4], cell division [3], sporulation [2, 5], stress response [6].

Recent studies reported that the eukaryotic-type serine/threonine kinase PrkC from *Bacillus subtilis* is also involved in bacterial exit from dormancy [7, 8]. Under conditions of nutritional limitation, *B. subtilis* produces dormant spores, which are resistant to harsh environmental conditions and can survive in a dormant state for years [7, 9-11]. The process of resuscitation is called, in these sporulating bacteria, germination [7, 8]. Generally, growing bacteria release muropeptides in the surrounding environment, due to cell wall peptidoglycan remodelling associated to cell growth and division [12, 13]. Therefore, the presence of muropeptides in the close environment of dormant spores is a clear signal that conditions are optimal for growth. Consistently, Shah el al. reported that m-Dpm-containing muropeptides are powerful germinants of *B. subtilis* spores [7]. Notably, other authors have independently proposed the idea that the activating ligand of PrkC could be a component or a degradation product of the cell wall peptidoglycan [6]. These authors also showed that, once activated, PrkC is able to phosphorylate the small ribosome-associated GTPase CpgA, the translation factor EF-Tu, and a component of the bacterial stressosome, denoted as YezB [6]. On the other hand, the possible involvement of the elongation factor EF-G as a substrate of PrkC is controversial [6, 7, 14].

A close homologue of PrkC exists in *Staphylococcus aureus*, a significant human pathogen that causes a number of infections ranging from skin infections to toxic shock syndrome, osteomyelitis and myocarditis [15, 16]. PrkC kinase from *S. aureus* is predicted to be a membrane protein, similar to its homologue from *B. subtilis* [2]. The two kinases present the same domain organisations, with an intracellular serine/threonine kinase domain, a transmembrane region, and an extra-cellular portion that contains three domains denoted as PASTA (Penicillin binding Associated and Serine/Threonine kinase Associated domains). Such domains also exist in penicillin binding proteins [17]. The crystal structure of the penicillin binding protein PBP2x from *S. peumoniae*, which contains two C-terminal PASTA domains, was solved in complex with cefuroxime, a β-lactam antibiotic mimicking the unlinked peptidoglycan [18, 19]. In this structure, cefuxomine binds one PASTA domain [18, 19], a finding which has suggested that PASTA domains of PrkC can bind muropeptides [7]. According to Shah et al., *B. subtilis* spores germinate in response to m-Dpm containing muropeptide, which constitute *B. subtilis* cell wall, but not in response to L-Lys containing muropeptide [7]. Moreover, when the PrkC from *B. subtilis* is substituted by PrkC from *S. aureus*, which is characterised by L-Lys containing cell walls, germination is observed both in response to m-Dpm and L-Lys containing muropeptide. This finding has shown that the source of PrkC determines the bacterial ability to respond to muropeptides and has suggested that PrkC extra-cellular domains exhibit specificity of muropeptide binding [7]. Despite these hypotheses, structural results are still needed to help the understanding of the function of extracellular domains.

To get insight into the mechanism of regulation of PrkC activity, mediated by the kinase extra-cellular domains, we undertook a structural study of the extra-cellular portion of PrkC from S.

aureus (EC-PrkC, residues 378-664, 33 kDa). The increase of *S. aureus* strains resistant methicillin, a β-lactam antibiotic of the penicillin class, makes infections particularly troublesome and difficult to treat in hospitals, where patients are at greater risk of infection than the general public. The present structural study provides a valuable template for the rational design of new anti-bacterial molecular entities able to interfere with cellular processes regulated by PrkC.

RESULTS

PrkC from *S. aureus* is a 664 residues long multidomain protein. Using sequence analysis tools, PrkC sequence is predicted to embed a Ser/Thr kinase domain (residues 1-270), a region of unknown structure and function (residues 271-377) that includes a transmembrane helix (residues 349-373), and an extra-cellular region, here denoted as EC-PrkC (residues 378-664). We determined the crystal structure of EC-PrkC, which is predicted to contain three successive PASTA domains (Figure 1A). We over-expressed this fragment of PkrC in *E. coli* and obtained a soluble form that was amenable for crystallisation. Since a sole methionine is present in the sequence of EC-PrkC, we tackled structure factor phasing by preparing derivatives of EC-PrkC crystals with several heavy metals. Best results were obtained with lantanides. Indeed, a Multi-wavelength Anomalous Diffraction (MAD) data collection using a lutetium-derivatised crystal, was performed at DESY, Hamburg, Germany. Diffraction data, at 2.9 Å resolution, allowed us to trace a significant part of the molecule [20]. Higher diffraction data (2.2 Å resolution) were collected in-house on a Europium-derivatised crystal. Using the Single-wavelength Anomalous Diffraction (SAD) method, these data produced a readily interpretable electron density throughout the entire structure. The final model contained 285 residues, five Europium ions, and 125 Water molecules. Data collection, refinement, and model statistics are summarised in Table 1.

The extra-cellular region of PrkC has the shape of a golf-stick

The crystal structure of EC-PrkC revealed that the extra-cellular region of PrkC consists of four consecutive domains. The four domains are arranged sequentially in a golf-stick shape, such that only neighbouring domains interact with each other (Figure 1B). Three of the four domains are, as predicted, PASTA domains (Figure 1A). The structure shows that the three PASTA domains display a linear and regular organisation. Indeed, each domain exhibits a twofold symmetry with respect to its neighbouring domains (Figure 1B). In this organisation, the sole α-helix of each domain is alternatively located on the two sides of the golf-stick (Figure 1B). Interestingly, the structure reveals the existence of a fourth domain, at the C-terminal end of the molecule, not predicted by searches in the PFAM database [21]. Furthermore, sequence analyses against the Protein Data Bank do not identify any significant homolog for this domain.

Three predicted PASTA

This work provides the highest resolution study of PASTA domains, which are arranged in βαββββ motifs (Figure 1B,D). Despite a moderate sequence identity between EC-PrkC PASTA domains (from 21 to 27%, Table 2), the structures of these domains are well conserved.

PASTA domains are constituents of the penicillin-binding PBP2x protein from *S. pneumoniae* [18]. The crystal structure of PBP2x shows that its two PASTA domains form a compact structure with a pronounced inter-domain bending (Figure 2). In this arrangement, each PASTA domain is involved in interactions with both the other PASTA domain and with the dimerisation and transpeptidase domains of PBP2x [18]. Differently, in the structure of EC-PrkC, the three PASTA domains are linearly arranged, with a limited number of inter-domain interactions. This finding suggests a high flexibility of the PrkC extra-cellular region.

The structural comparison of PrkC PASTA domains with those of PBP2x shows a significant conservation of the PASTA fold, despite the low sequence identities, ranging from 5 to 28%, between domains (Table 2). All secondary structure elements are conserved, although β-strands β4 and β5 do not appear in lower resolution PBP2x structures [22]. Despite an overall conservation of the fold, however, EC-PrkC PASTA domains present a six-residue insertion between β-strands β2 and β3 (YSDKYP, YNNQAP, YSDDID for PASTA 1, 2, and 3, respectively). Furthermore, a Ser-X-Gly motif, which does not exist in PBP2x, occurs at the C-terminal end of each PASTA domain. This sequence motif is conserved in many homologous bacterial proteins (Figure S1). In each PASTA domain of EC-PrkC crystal structure, the serine side chain (Ser508 in PASTA2, Figure 2B) of the Ser-X- Gly motif establishes a hydrogen bond with the backbone nitrogen of glycine (Gly510

in PASTA2) and with the carbonyl oxygen of a neighbouring residue (Ala480 in PASTA2) (Figure2B). These interactions may play a role in keeping a linear arrangement of PASTA domains. Conversely, a contribution to compact head-to-tail arrangement of PBP2x PASTA domains likely comes from their tertiary structure interactions with the rest of the protein structure (Figure 2C).

While this work was in preparation, the solution NMR structure of three overlapping sequences of PknB from *M. tuberculosis*, each embedding two PASTA domains, and the small-angle X-ray scattering study of the entire extra-cellular PknB portion (four PASTA domains) appeared [23]. Unlike PBP2x, the organisation of PASTA domains in the PknB structure is nearly linear [18, 23]. However, the overall RMSD calculated on Cα atoms after superposition of the three PASTA domains of EC-PrkC with those of PknB is as high as 9.5 Å (after superposition with PknB PASTA domains 2, 3 and 4) and 14.4 Å (after superposition with PknB PASTA domains 1, 2 and 3). This is mainly due to different arrangements of PASTA domains in PrkC and PknB (Figure 3). Indeed, when single PASTA domains of EC-PrkC and PknB are superposed, a strong conservation of the domain fold is observed, even in cases when sequence identities are as low as 2-5% (Table 2). Based on the observation that the two PASTA domains of PBP2x interact with each other (Figure 2C) [18], the authors proposed that extra-cellular regions of PknB dimerise to activate the kinase, since only dimerisation would bring two PASTA domains in close contact [23]. However, it should be noted that the two PASTA domains of PBP2x are oriented in opposite directions (Figure 2A). Therefore, similar interactions would produce PknB dimers that would not allow the catalytic domains to interact (See Discussion).

PrkC C-terminal domain: an IG-like domain with a missing strand

The PrkC C-terminal domain (residues 577-664) exhibits an all-beta structure, which contains six β-strands arranged in a beta sandwich (Figure 1C). Sequence alignment analyses do not identify any structure in the PDB with significant sequence identity. However, a DALI [24] search of the Protein Data Bank (PDB) reveals that PrkC C-terminal domain structurally resembles a set of Immunoglobulin (IG) domains (Table 3). The canonical structure of IG domains is formed by a three-stranded and a four-stranded β-sheet packed in β-sandwich arrangement [25]. Like canonical IG domains, PrkC IG domain (PrkC-IG) presents a hydrophobic core formed by both β-sheets, whereas residues pointing to the solvent are mainly hydrophilic; this results in alternating polar/unpolar sequence patterns of the β-strands. The topology of PrkC-IG can be classified as belonging to the s-type IG domains [25]. However, superposition of PrkC-IG to those identified with DALI (Table 3) shows that this domain misses the N-terminal strand (β-strand β* of the canonical IG domain, Figure 1C). The sole identified protein that shares a similar feature is a type III domain of human fibronectin (PDB code 2h41, Table 3). In EC-PrkC, the N-terminal missing strand of PrkC-IG forms the linker with the PASTA3 domain (Figure 1). Different from typical IG folds, where hydrophobic residues in the β* strand pack against the hydrophobic core, PrkC linker is highly hydrophilic. The volume occupied by hydrophobic residues of the β* strand in canonical IG domains is filled by bulky hydrophilic residues of β-strands β1 and β6 in EC-PrkC (data not shown).

It is worth noting that IG domains similar to PrkC-IG are usually involved in cell-cell interactions and cell signalling [26]. Their adhesive properties are exploited both by bacterial [27, 28] and eukaryotic cells [29] and are typically due to the exposure of an anomalously large number of backbone β-strand hydrogen-bond donors and acceptors [30]. This is particularly true when IG folds are not complete and miss one β-strand (as in PrkC-IG, Figure 1C), since this feature leads in extreme cases to IG polymerisation [31, 32]. These properties of PrkC-IG suggest that this domain may also play a role in peptidoglycan binding, in a fashion similar to the *E. coli* adhesin PapG with host glycolypids [33, 34]. Consistently, we noted that *B. subtilis* PrkC, which from shares similar properties in inducing bacterial sporulation, also contains a similar domain at its C-terminus.

EC-PrkC oligomerisation state in the crystal state and in solution

Analysis of packing interactions between symmetry-related molecules of EC-PrkC crystal structure, using the software PISA [35], evidenced no strong protein interfaces that would anticipate the existence of an oligomeric form of the protein. Given the importance of dimerisation in the activation of several kinases [26, 36], we decided to check it using several techniques and experimental conditions.

Gel filtration profiles of freshly purified EC-PrkC showed the existence of a species with molecular weight of about 66 kDa, compatible with a dimeric arrangement of the protein (Figure S2). However, estimates of molecular weights by gel filtration depend on the protein shape and abnormal values are calculated for non-globular elongated molecules.

Therefore, we used analytical size-exclusion chromatography (SEC), coupled with multiangle light scattering (MALS). MALS is a powerful tool to characterise the weight average molar mass (Mw) of compounds showing anomalous elution profiles in SEC. The on-line measurement of the intensity of the Rayleigh scattering as a function of the angle as well as the differential refractive index of the eluting peak in SEC was used to determine Mw. This analysis produced an Mw value of 31060 ±620 Da, which corresponds to a monomeric organisation of the molecule (Figure 4). In parallel, SEC-MALS experiments were carried out after overnight incubation of EC-PrkC with a mixture blend of natural muropeptides (Table 4). Results, which provided an Mw value of 31120 ± 311 Da, clearly showed that the protein retains its monomeric state also in the presence of a large excess of muropeptides (Figure 4).

Furthermore, to check if the molecular size distribution of EC-PrkC changes at increasing protein concentrations, we also performed Dynamic Light Scattering (DLS). This analysis was carried out at 25 °C using protein concentrations ranging from 1.0 to 6.0 mg/mL. In all conditions, a population of 2.8 ± 0.3 nm hydrodynamic radii (Rh) particles dominated and no significant variations of Rh values were observed as a function of concentration. Similarly, we measured the molecule Rh after its incubation with a 4-molar excess of natural muropeptides mixture (Table 4). As a result, we observed no significant variation of Rh. Therefore, high concentrations do not induce EC-PrkC dimerisation, also after incubation with muropeptides.

The possible formation of a complex deriving from self-recognition and the effect of muropeptides on this process were also evaluated using Surface Plasmon Resonance. Real Time binding assays were performed on a Biacore 3000 Surface Plasmon Resonance (SPR) instrument. EC-PrkC was immobilised using two different methods to ensure different experimental conditions and protein orientations on the chip: on a CM5 sensor chip by covalent EDC-NHS amine coupling and on an NTA (nitrilotriacetic acid) sensor chip, which immobilises the protein N-terminal His-tag on NTA-chelated nickel of the chip. Furthermore, to investigate the effect of the ligand concentration on potential protein-protein interactions, we used two immobilisation levels (See Methods).

In both experiments, EC-PrkC was injected as analyte at concentrations ranging from 1.0 to 100 µM. The possible effect of muropeptides on protein-protein interaction was evaluated by injecting EC-PrkC after pre-incubation with the muropeptides mixture (Table 4) from 0 to 100 equivalents. As a result, no significant RU variation was observed in all SPR assays (Figure S3). These results confirmed those obtained by SEC-MALS and DLS, that EC-PrkC has no tendency to self-aggregate and that muropeptides do not induce EC-PrkC dimerisation.

DISCUSSION

We present here the x-ray structure characterisation of the entire extra-cellular region of the Ser/Thr kinase PrkC from *S. aureus*, EC-PrkC. This kinase has been shown to signal peptidoglycan-induced revival of *B. subtilis* from dormancy, similar to *B. subtilis* endogenous PrkC [7]. The mechanism of peptidoglycan-induced activation of PrkC is, however, so far unknown.

We show that of EC-PrkC adopts an elongated structure composed of four domains: three PASTA domains and a C-terminal domain, which was not predicted by searches in the PFAM database (Figure 1A). This latter domain, here denominated PrkC-IG, structurally resembles an Immunoglobulin (IG) fold, despite the low sequence identity with IG folds in the PDB. It is worth noting that PrkC from *S. aureus* and from *B. subtilis* share the same domain architecture and a reasonable sequence identity (about 27%). A domain similar to *S. aureus* PrkC-IG exists also in PrkC from *B. subtilis*, as suggested by the significantly high sequence identity (30%) between the C-terminal regions of the two homologous proteins. Therefore, it is not surprising that PrkC from the two bacteria induce similar responses in terms of germination of *B. subtilis* spores [7].

The kinase domain of PrkC from *S. aureus* is homologous to that of the serine/threonine kinase PknB from *M. tuberculosis* (37% sequence identity). Similar to PknB [37] and to PrkC from *B. subtilis* [5], the kinase domain of PrkC from *S. aureus* undergoes auto-phosphorylation [38]. Furthermore, the x-ray structure of the kinase domain of PknB suggests a model in which a structural and functionally asymmetric "front-to-front" association occurs. This dimerisation mode leads to the phosphorylation of serine and threonine residues located in the kinase activation loop [37]. Therefore, the most obvious mechanism to explain the muropeptide-driven activation of PrkC involves the muropeptide-induced dimerisation of the PrkC extra-cellular region that leads to the formation of the asymmetric, active, PrkC dimer.

Dimerisation is a typical event that activates kinases, since it permits auto-phosphorylation. However, the structural basis of this phenomenon may be different. Indeed, dimerisation can either be intrinsic, although stabilised by the activating ligand, or entirely induced by the activating ligand [26]. Our data demonstrate that PrkC extra-cellular region displays no intrinsic tendency to dimerise (Figure 4) and that the sole muropeptide fails to induce dimerisation even in the presence of a large muropeptide excess (Figures 4 and S3). It is worth noting that the extra-cellular region and, to a smaller extent, the trans-membrane region of PrkC from B. subtilis are able to form dimers *in vivo* [2]. Therefore, our data point to a more complex dimerisation mechanism, which may require the contribution of the trans-membrane domain [2] and may be only indirectly modulated by muropeptides.
Furthermore, the dimerisation of the extra-cellular PrkC observed *in vivo* [2] may involve of a third molecule, yet unknown, in a fashion similar to that observed for the fibroblast growth factor receptor (FGFR)[39]. Indeed, dimerisation of FGFR involves three IG-like domains (domains D1-D3) and requires the simultaneous participation of both a fibroblast growth factor receptor (FGF) and heparin, through the formation of a ternary complex [26, 39]. It cannot be excluded, however, as previously observed for other kinase receptors [40], that the binding of the sole muropeptide molecule is not sufficient induce dimerisation, but it stabilises a conformation of the extra-cellular region that favours the dimerisation of the entire molecule. Finally, our work provides a high-resolution structure of the extra-cellular, and therefore accessible to drugs, region of PrkC. As such, they will be precious to r aimed at the development of novel anti-bacterial molecular entities able to interfere with processes involving PrkC.

EXPERIMENTAL PROCEDURES

Protein expression and purification. The plasmidic construct corresponding to the extra-cellular PrkC of *S. aureus* (EC-PrkC, residues 378-664) has been prepared as previously described by Dworkin et al. [7]. The overexpression of EC-PrkC, containing an N-terminal histidine tag (His_6) was carried using *E. coli* DH5α cells (Invitrogen), as described [20]. Purification was performed by affinity chromatography, using a 5-mL Ni-NTA column (GEHelthcare). A further purification step included gel filtration, on a Superdex 200 column (GeHelthcare), equilibrated in 150 mM NaCl, 20 mM TrisHCl buffer at pH 8.0 and 5% (v/v) glycerol. The protein, which eluted in a single peak, was concentrated using a centrifugal filter device (Millipore), and the concentration was determined by Bradford protein assay (Biorad). Fresh concentrated protein at 10 mg mL^{-1}, was used for crystallisation experiments.

Crystallisation, data collection and processing. Crystallisation trials were performed at 293 K using the hanging-drop vapor-diffusion method. Preliminary crystallisation conditions were set up using a robot station for high throughput crystallisation screening (Hamilton STARlet NanoJet 8+1) and commercially available sparse-matrix kits (Crystal Screen kits I and II, Hampton Research, Index). Optimisation of the crystallisation conditions was performed manually both using the vapor-diffusion and the macro-seeding technique. Lutetium chloride derivative crystals were prepared by soaking a native crystal in a solution containing 1-3 mM lutetium chloride, 25% (w/v) MPEG2000, 160 mM ammonium sulphate, 60 mM sodium acetate trihydrate buffer for 3 hours at pH 4.6. A Multi-wavelength Anomalous Diffraction experiment (MAD) was carried out on a crystal derivatised with 2mM $LuCl_3$ at the X12 synchrotron beam line, DORIS storage ring, DESY (Hamburg, Germany), at 100 K. Cryoprotection of the crystals was achieved by a fast soaking in a solution containing glycerol to a final concentration of 10% (v/v). These data, extending to 3.0 Å resolution, allowed us to build a part of the molecule [20]. Derivatisation by overnight soaking in a solution containing 2mM Europium chloride provided higher resolution x-ray data, at 2.2 Å (Table 1). Data collection was performed in-house at 100K using a Rigaku Micromax 007 HF generator producing Cu $K\alpha$ radiation and equipped with a Saturn944 CCD detector. The data sets were scaled and merged using HKL2000 program package [41] (Table 1).

Structure determination. Initial phasing was performed on MAD x-ray data using the Auto-Rickshaw platform using the anomalous signal from the Lu3+ ions [42]. Better phasing was achieved using in-house Single Anomalous Dispersion data, collected on a crystal soaked overnight in a solution containing 2mM Europium chloride. These data provided structure factors phases to 2.2 Å resolution. Both SHELXD [43] and SOLVE identified five Europium ions. Phases, improved by phase extension and density modification by RESOLVE [44] and wARP [45] allowed us to trace nearly the entire molecule structure. Crystallographic refinement was carried out against 95% of the measured data using the CCP4 program suite [46]. The remaining 5% of the observed data, which was randomly selected, was used in Rfree calculations to monitor the progress of refinement. Structures were validated using the program PROCHECK [47].

Bioinformatic analysis. A set of tools was used to analyse the structural characteristics of PrkC. The database PFAM was searched to assign the domain organisation of the enzyme. BLAST searches were performed to look for possible structures with significant sequence identity. Trans-membrane regions were searched using TMPRED and TMHMM [48, 49].

Multiple Angle Light Scattering experiments. Purified EC-PrkC was analysed by size-exclusion chromatography (SEC) coupled to a DAWN MALS instrument (Wyatt Technology) and an OptilabTM rEX (Wyatt Technology). 600 µg of sample was loaded a S200 10/30 column, equilibrated in 50 mM Tris–HCl, pH 8.0 and 0.15 M NaCl. A constant flow rate of 0.5 mL/min was applied. The on-line measurement of the intensity of the Rayleigh scattering as a function of the angle as well as the differential refractive index of the eluting peak in SEC was used to determine the weight average molar mass (Mw) eluted proteins, using the Astra 5.3.4.14 software (Wyatt Technologies). To check if the oligomerisation state of EC-PkrC changed upon binding of muropeptides, 600 µg of sample was incubated overnight with 10-molar excess of a mixture blend

of natural muropeptides at room temperature. The protein-muropeptide mixture was then analysed by SEC-MALS in the same conditions used for the protein alone.

In batch mode, samples were prepared at room temperature in 50 mM Tris–HCl, 150 mM NaCl buffer, pH 8.0. A stock solution of EC-PrkC was filtered through a 0.02 μm Millex syringe driven filter unit (Millipore, Bedford, MA). After a further measure of protein concentration, samples were prepared at concentrations ranging between 2.5 and 5.0 mg/ml. All measurements were registered in triplicates for 2 min acquisition time. The hydrodynamic radius (Rh) of the scattering molecules was derived, using the ASTRA software, from the diffusion coefficient from the Einstein–Stokes equation.

Surface Plasmon Resonance experiments. Real Time binding assays were performed on a Biacore 3000 Surface Plasmon Resonance (SPR) instrument using two different sensor chips. Covalent immobilisation of EC-PrkC on a CM5 sensor chip was carried out with EDC-NHS amine coupling chemistry in 10 mM acetate buffer pH 4.0. In parallel, the N-terminal His-tag of EC-PrkC was immobilised on NTA sensor chip (flow rate 5 μL/min, injection time 7 min). In the covalent CM5 immobilisation, residual reactive groups were deactivated by treatment with 1 M ethanolamine hydrochloride, pH 8.5. The reference channel was prepared by activating with EDC/NHS and deactivating with ethanolamine.

SPR experiments were performed with two different immobilisation levels: 2800 and 1000 RU in CM5 covalent immobilisation and 1063 and 364 RU in NTA His-tag capturing. A stock EC-PrkC solution was diluted in running buffer HBS (10 mM Hepes, 150 mM NaCl, 3 mM EDTA, pH 7.4) and injected as analyte (flow rate 20 μL/min, injection volume 90 μL) at various concentrations in the range 1.0-100 μM. In parallel, EC-PrkC was pre-incubated with a mixture of natural muropeptides (Table 4), in the concentration range from 0 to 100 equivalents. As a control experiment, the muropeptide blend mixture (Table 4) was also injected as analyte.

Bacterial growth and purification of peptidoglycan. Dried cells of *E. coli* containing m-Dpm-type peptidoglycan were extracted as described elsewhere [50]. Briefly, cells were suspended in ice-cold water, added drop-wise to boiling 8% SDS and boiled for 30 min. After cooling down to room temperature, the SDS-insoluble material was collected by centrifugation. The pellets were washed several times with water until no SDS could be detected. High molecular weight glycogen and covalently bound lipoprotein were removed by treatment with α-amylase and trypsin. Further sequential washes with 8 M LiCl, 0.1M EDTA and acetone were sequentially performed.

Preparation of muropeptides, GC-MS, HPLC and LC-MS analyses. The isolated peptidoglycan was degraded with muramidase mutanolysin from *Streptomyces globisporus* ATCC21553 (Sigma-Aldrich) at 37°C overnight. The enzyme reaction was stopped by boiling (5 min), and insoluble contaminants were removed by centrifugation.

The generated muropeptides were dissolved in 0.5 M sodium borate buffer, pH 9.0 and solid sodium borohydride was added immediately. After incubation for 30 min at room temperature, excess borohydride was destroyed with HCl 2M. Finally, the samples were adjusted to pH 3-4 with TFA. Reduced muropeptides were fractionated by reverse phase HPLC [50]. Briefly, the muropeptides were eluted with a linear gradient (run time 40 min) from 0 to 17.5% acetonitrile. Detection was by A_{206} nm whereas identification was achieved by ESI+ MS and ESI-/MS spectra in 2% formic acid-methanol 1:1 v/v and water-methanol 1:1 v/v, respectively (Agilent 1100MSD) as described [51].

ACCESSION NUMBERS. Coordinates and structure factors have been deposited in the Protein Data Bank with accession number 3py9.

SUPPLEMENTAL INFORMATION. Supplemental Information includes three Supplemental figures and can be found with this article online at doi:xxx.

ACKNOWLEDGMENTS

We would like to thank Prof. Jonathan Dworkin for providing EC-PrkC clone and Dr. Viviana Izzo and Ms. Luisa Palamara for their kind help in setting protein expression conditions. We acknowledge assistance from the EMBL staff (beamline X12, Hamburg, Germany). We also

acknowledge COST action BM1003 "*Microbial cell surface determinants of virulence as targets for new therapeutics in Cystic Fibrosis*".

References

1 Munoz-Dorado, J., Inouye, S. and Inouye, M. (1991) A gene encoding a protein serine/threonine kinase is required for normal development of M. xanthus, a gram-negative bacterium. Cell **67**, 995-1006

2 Madec, E., Laszkiewicz, A., Iwanicki, A., Obuchowski, M. and Seror, S. (2002) Characterization of a membrane-linked Ser/Thr protein kinase in Bacillus subtilis, implicated in developmental processes. Mol Microbiol **46**, 571-86

3 Fiuza, M., Canova, M. J., Zanella-Cleon, I., Becchi, M., Cozzone, A. J., Mateos, L. M., Kremer, L., Gil, J. A. and Molle, V. (2008) From the characterization of the four serine/threonine protein kinases (PknA/B/G/L) of Corynebacterium glutamicum toward the role of PknA and PknB in cell division. J Biol Chem **283**, 18099-112

4 Fiuza, M., Canova, M. J., Patin, D., Letek, M., Zanella-Cleon, I., Becchi, M., Mateos, L. M., Mengin-Lecreulx, D., Molle, V. and Gil, J. A. (2008) The MurC ligase essential for peptidoglycan biosynthesis is regulated by the serine/threonine protein kinase PknA in Corynebacterium glutamicum. J Biol Chem **283**, 36553-63

5 Madec, E., Stensballe, A., Kjellstrom, S., Cladiere, L., Obuchowski, M., Jensen, O. N. and Seror, S. J. (2003) Mass spectrometry and site-directed mutagenesis identify several autophosphorylated residues required for the activity of PrkC, a Ser/Thr kinase from Bacillus subtilis. J Mol Biol **330**, 459-72

6 Absalon, C., Obuchowski, M., Madec, E., Delattre, D., Holland, I. B. and Seror, S. J. (2009) CpgA, EF-Tu and the stressosome protein YezB are substrates of the Ser/Thr kinase/phosphatase couple, PrkC/PrpC, in Bacillus subtilis. Microbiology **155**, 932-43

7 Shah, I. M., Laaberki, M. H., Popham, D. L. and Dworkin, J. (2008) A eukaryotic-like Ser/Thr kinase signals bacteria to exit dormancy in response to peptidoglycan fragments. Cell **135**, 486-96

8 Shah, I. M. and Dworkin, J. (2010) Induction and regulation of a secreted peptidoglycan hydrolase by a membrane Ser/Thr kinase that detects muropeptides. Mol Microbiol, In the press.

9 Kana, B. D. and Mizrahi, V. (2010) Resuscitation-promoting factors as lytic enzymes for bacterial growth and signaling. FEMS Immunol Med Microbiol **58**, 39-50

10 Warner, D. F. and Mizrahi, V. (2007) The survival kit of Mycobacterium tuberculosis. Nat Med **13**, 282-4

11 Keep, N. H., Ward, J. M., Cohen-Gonsaud, M. and Henderson, B. (2006) Wake up! Peptidoglycan lysis and bacterial non-growth states. Trends Microbiol **14**, 271-6

12 Hett, E. C. and Rubin, E. J. (2008) Bacterial growth and cell division: a mycobacterial perspective. Microbiol Mol Biol Rev **72**, 126-56

13 Ruggiero, A., Marasco, D., Squeglia, F., Soldini, S., Pedone, E., Pedone, C. and Berisio, R. (2010) Structure and functional regulation of RipA, a mycobacterial enzyme essential for daughter cell separation. Structure **18**, 1184-90

14 Gaidenko, T. A., Kim, T. J. and Price, C. W. (2002) The PrpC serine-threonine phosphatase and PrkC kinase have opposing physiological roles in stationary-phase Bacillus subtilis cells. J Bacteriol **184**, 6109-14

15 McGahee, W. and Lowy, F. D. (2000) Staphylococcal infections in the intensive care unit. Semin Respir Infect **15**, 308-13

16 Ohlsen, K. and Donat, S. (2010) The impact of serine/threonine phosphorylation in Staphylococcus aureus. Int J Med Microbiol **300**, 137-41

17 Yeats, C., Finn, R. D. and Bateman, A. (2002) The PASTA domain: a beta-lactam-binding domain. Trends Biochem Sci **27**, 438

18 Gordon, E., Mouz, N., Duee, E. and Dideberg, O. (2000) The crystal structure of the penicillin-binding protein 2x from Streptococcus pneumoniae and its acyl-enzyme form: implication in drug resistance. J Mol Biol **299**, 477-85

19 Dessen, A., Mouz, N., Gordon, E., Hopkins, J. and Dideberg, O. (2001) Crystal structure of PBP2x from a highly penicillin-resistant Streptococcus pneumoniae clinical isolate: a mosaic framework containing 83 mutations. J Biol Chem **276**, 45106-12

20 Ruggiero, A., Squeglia, F., Izzo, V., Silipo, A., Vitagliano, L., Molinaro, A. and Berisio, R. (2010) Expression, Purification, Crystallization and Preliminary X-Ray Crystallographic Analysis of the Peptidoglycan Binding Region of the Ser/Thr Kinase PrkC from Staphylococcus aureus. Protein Pept Lett, In the press

21 Finn, R. D., Tate, J., Mistry, J., Coggill, P. C., Sammut, S. J., Hotz, H. R., Ceric, G., Forslund, K., Eddy, S. R., Sonnhammer, E. L. and Bateman, A. (2008) The Pfam protein families database. Nucleic Acids Res **36**, D281-8

22 Pares, S., Mouz, N., Petillot, Y., Hakenbeck, R. and Dideberg, O. (1996) X-ray structure of Streptococcus pneumoniae PBP2x, a primary penicillin target enzyme. Nat Struct Biol **3**, 284-9

23 Barthe, P., Mukamolova, G. V., Roumestand, C. and Cohen-Gonsaud, M. (2010) The structure of PknB extracellular PASTA domain from mycobacterium tuberculosis suggests a ligand-dependent kinase activation. Structure **18**, 606-15

24 Holm, L. and Sander, C. (1995) Dali: a network tool for protein structure comparison. Trends Biochem Sci **20**, 478-80

25 Bork, P., Holm, L. and Sander, C. (1994) The immunoglobulin fold. Structural classification, sequence patterns and common core. J Mol Biol **242**, 309-20

26 Lemmon, M. A. and Schlessinger, J. (2010) Cell signaling by receptor tyrosine kinases. Cell **141**, 1117-34

27 Bowden, M. G., Heuck, A. P., Ponnuraj, K., Kolosova, E., Choe, D., Gurusiddappa, S., Narayana, S. V., Johnson, A. E. and Hook, M. (2008) Evidence for the "dock, lock, and latch" ligand binding mechanism of the staphylococcal microbial surface component recognizing adhesive matrix molecules (MSCRAMM) SdrG. J Biol Chem **283**, 638-47

28 Ganesh, V. K., Rivera, J. J., Smeds, E., Ko, Y. P., Bowden, M. G., Wann, E. R., Gurusiddappa, S., Fitzgerald, J. R. and Hook, M. (2008) A structural model of the Staphylococcus aureus ClfA-fibrinogen interaction opens new avenues for the design of anti-staphylococcal therapeutics. PLoS Pathog **4**, e1000226

29 Carafoli, F., Saffell, J. L. and Hohenester, E. (2008) Structure of the tandem fibronectin type 3 domains of neural cell adhesion molecule. J Mol Biol **377**, 524-34

30 Richardson, J. S. and Richardson, D. C. (2002) Natural beta-sheet proteins use negative design to avoid edge-to-edge aggregation. Proc Natl Acad Sci U S A **99**, 2754-9

31 Kline, K. A., Dodson, K. W., Caparon, M. G. and Hultgren, S. J. (2010) A tale of two pili: assembly and function of pili in bacteria. Trends Microbiol **18**, 224-32

32 Vitagliano, L., Ruggiero, A., Pedone, C. and Berisio, R. (2007) A molecular dynamics study of pilus subunits: insights into pilus biogenesis. J Mol Biol **367**, 935-41

33 Dodson, K. W., Pinkner, J. S., Rose, T., Magnusson, G., Hultgren, S. J. and Waksman, G. (2001) Structural basis of the interaction of the pyelonephritic E. coli adhesin to its human kidney receptor. Cell **105**, 733-43

34 Imberty, A., Mitchell, E. P. and Wimmerova, M. (2005) Structural basis of high-affinity glycan recognition by bacterial and fungal lectins. Curr Opin Struct Biol **15**, 525-34

35 Krissinel, E. and Henrick, K. (2007) Inference of macromolecular assemblies from crystalline state. J Mol Biol **372**, 774-97

36 Chung, I., Akita, R., Vandlen, R., Toomre, D., Schlessinger, J. and Mellman, I. (2010) Spatial control of EGF receptor activation by reversible dimerization on living cells. Nature **464**, 783-7

37 Mieczkowski, C., Iavarone, A. T. and Alber, T. (2008) Auto-activation mechanism of the Mycobacterium tuberculosis PknB receptor Ser/Thr kinase. Embo J **27**, 3186-97

38 Debarbouille, M., Dramsi, S., Dussurget, O., Nahori, M. A., Vaganay, E., Jouvion, G., Cozzone, A., Msadek, T. and Duclos, B. (2009) Characterization of a serine/threonine kinase involved in virulence of Staphylococcus aureus. J Bacteriol **191**, 4070-81

39 Schlessinger, J., Plotnikov, A. N., Ibrahimi, O. A., Eliseenkova, A. V., Yeh, B. K., Yayon, A., Linhardt, R. J. and Mohammadi, M. (2000) Crystal structure of a ternary FGF-FGFR-heparin complex reveals a dual role for heparin in FGFR binding and dimerization. Mol Cell **6**, 743-50

40 D'Andrea, L. D., Iaccarino, G., Fattorusso, R., Sorriento, D., Carannante, C., Capasso, D., Trimarco, B. and Pedone, C. (2005) Targeting angiogenesis: structural characterization and biological properties of a de novo engineered VEGF mimicking peptide. Proc Natl Acad Sci U S A **102**, 14215-20

41 Otwinowski, Z. and Minor, W. (1997) Methods Enzymol. **276**, 307–326

42 Panjikar, S., Parthasarathy, V., Lamzin, V. S., Weiss, M. S. and Tucker, P. A. (2005) Auto-Rickshaw: an automated crystal structure determination platform as an efficient tool for the validation of an X-ray diffraction experiment. Acta Crystallogr D Biol Crystallogr **61**, 449-57

43 Sheldrick, G. M. (2008) A short history of SHELX. Acta Crystallogr A **64**, 112-22

44 Terwilliger, T. (2004) SOLVE and RESOLVE: automated structure solution, density modification and model building. J Synchrotron Radiat **11**, 49-52

45 Langer, G., Cohen, S. X., Lamzin, V. S. and Perrakis, A. (2008) Automated macromolecular model building for X-ray crystallography using ARP/wARP version 7. Nat Protoc **3**, 1171-9

46 Potterton, E., Briggs, P., Turkenburg, M. and Dodson, E. (2003) A graphical user interface to the CCP4 program suite. Acta Crystallogr D Biol Crystallogr **59**, 1131-7

47 Laskowski, R. A., Rullmannn, J. A., MacArthur, M. W., Kaptein, R. and Thornton, J. M. (1996) AQUA and PROCHECK-NMR: programs for checking the quality of protein structures solved by NMR. J Biomol NMR **8**, 477-86

48 Hu, J. and Yan, C. (2008) HMM_RA: an improved method for alpha-helical transmembrane protein topology prediction. Bioinform Biol Insights **2**, 67-74

49 Bertaccini, E. and Trudell, J. R. (2002) Predicting the transmembrane secondary structure of ligand-gated ion channels. Protein Eng **15**, 443-54

50 Girardin, S. E., Boneca, I. G., Carneiro, L. A., Antignac, A., Jehanno, M., Viala, J., Tedin, K., Taha, M. K., Labigne, A., Zahringer, U., Coyle, A. J., DiStefano, P. S., Bertin, J., Sansonetti, P. J. and Philpott, D. J. (2003) Nod1 detects a unique muropeptide from gram-negative bacterial peptidoglycan. Science **300**, 1584-7

51 Erbs, G., Silipo, A., Aslam, S., De Castro, C., Liparoti, V., Flagiello, A., Pucci, P., Lanzetta, R., Parrilli, M., Molinaro, A., Newman, M. A. and Cooper, R. M. (2008) Peptidoglycan and muropeptides from pathogens Agrobacterium and Xanthomonas elicit plant innate immunity: structure and activity. Chem Biol **15**, 438-48

Figure Captions

Figure 1. The modular structure pf EC-PrkC. (A) Domains prediction of PrkC, according to the PFAM database. IC-PrkC and EC-PrkC are for intra-cellular and extra-cellular regions of PrkC, respectively. (B) Ribbon representation EC-PrkC. Helices and β -strands are reported in orange and blue, respectively. (C) Sketch of canonical IG domain topology. The grey strand in the topology sketch (strand β*) is missing in PrkC-IG. (D) Sketch of PASTA domain topology.

Figure 2. A comparison of EC-PrkC with PBP2x. (A) Superposition of the PASTA domain 1 of PBP 2x (PBP2x-1, orange, PDB code 1qme) with the PASTA domain 2 of PrkC (purple). (B) An enlargement of the insertion loop of PrkC PASTA2 and hydrogen bonding interactions mediated by Ser 508. (C) Top view of PBP2x structure; The ribbon and surface representations of PASTA domains are coloured in orange whereas representations of the rest of the molecule are shown in green.

Figure 3. A comparison of EC-PrkC with PknB. **(**A) Ribbon representation of the x-ray structure of EC-PrkC. (B) Ribbon representation of PASTA domain arrangement in PknB, as derived by SAXS studies, PDB code 1KUI. (C) Superposition of PknB PASTA domain 1 (light grey) with PrkC PASTA domain 2 (dark grey).

Figure 4. Analytical SEC-MALS of EC-PrkC. Rayleigh ratios and molecular masses (left and right scales, respectively) are plotted against the elution time. The black curve corresponds to EC-PrkC in 0.15 M NaCl and 50 mM Tris–HCl, pH 8.0. The grey curve was measured in the same buffer after overnight incubation of EC-PrkC with 10-molar excess muropeptides. In both experiments, average Mw values correspond to a monomeric state of the protein.

Table1. Data collection and refinement statistics

A. *Data collection*	
Space group	$P2_12_12$
Unit-cell parameters *a, b, c* (Å)	55.64, 69.40, 88.62
Resolution shell (Å)	30.0-2.2
N. of unique reflections	18045
Average redundancy	8.0 (8.0)
R_{merge}	0.08 (0.44)
Completeness (%)	99.9 (99.9)
Mean I/σ(I)	32.4 (3.8)
B. *Refinement*	
Resolution range (Å)	15.0-2.2
Rwork	0.210
Rfree	0.257
No. atoms	
Protein	2195
Water	125
Average ADPs (Å^2)	
Protein main chain, side chain	38.2, 41.9
Water	43.6
r.m.s. deviations	
Bond lengths (Å)	0.01
Bond angles (°)	1.56

Values in parentheses are for the highest resolution shell (2.28-2.20 Å)

Table 2. Structural comparison, as computed using DALI, of PrkC PASTA domains (PASTA1, PASTA2, PASTA3) with those of PBP2x (the two domains are denoted as PBP2x-1 and PBP2x-2) and of PknB (the four domains are denoted as MTB-P1 – MTB-P4).

		PASTA1	PASTA2	PASTA3	PBP2x-1	PBP2x-2	MTB-P1	MTB-P2	MTB-P3	MTB-P4
PASTA1	Z-score	10.7	10.1	7.2	7.8	6.1	7.8	9.8	6.3	
	Rmsd (Å)	1.2	1.7	2.2	2.1	3.1	2.1	1.5	3.0	
	Seq. id (%)	24	27	13	20	28	25	28	17	
PASTA2			10.7	8.0	7.2	5.9	8.0	2.0	7.9	
			1.7	2.1	2.2	2.8	1.9	2.8	2.9	
			21	13	26	23	21	2	20	
PASTA3				8.3	7.2	7.1	7.9	2.1	6.6	
				3.6	2.0	8.6	1.5	3.1	3.0	
				5	13	22	18	4	19	

Table 3. Structural comparison of PrkC IG domain with those, identified using DALI, with the highest structural similarity (Z-score > 5).

Description	PDB code	Z-score	Rmsd (Å)	Sequence identity (%)
Intercellular adhesion molecule ICAM-1	1mq8	5.1	2.6	13
Sulphur covalently binding protein	2nnf	5.3	2.4	21
Neural cell wall adhesion molecule	2vkx	5.3	3.2	6
Tenascin	3b83	5.2	2.6	9
Fibronectin	2h41	5.1	2.6	9

Table 4. Composition of the muropeptide blend mixture based on HPLC elution profiles and MS data.

m/z	Muropeptide composition
871.21	$GlcNAc_1MurNAc_1Ala_1Glu_1Dpm_1$
942.34	$GlcNAc_1MurNAc_1Ala_2Glu_1Dpm_1$
1722.20	$GlcNAc_2MurNAc_2Ala_2Glu_2Dpm_2$
1315.41	$GlcNAc_1MurNAc_1Ala_3Glu_2Dpm_2$
1794.12	$GlcNAc_2MurNAc_2Ala_3Glu_2Dpm_2$
1864.06	$GlcNAc_2MurNAc_2Ala_4Glu_2Dpm_2$

Biochemical Journal Immediate Publication. Published on 06 Jan 2011 as manuscript BJ20101643

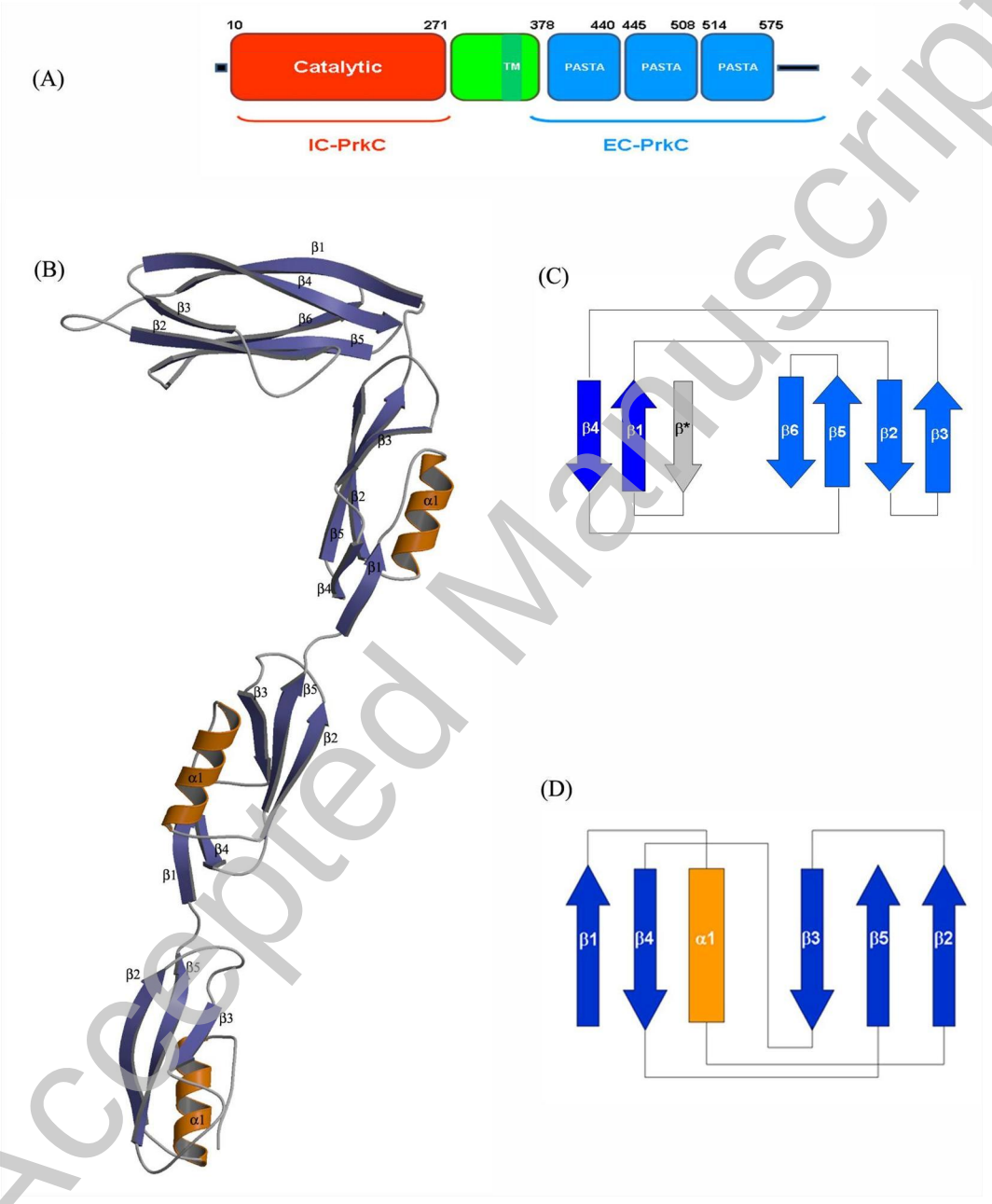

Biochemical Journal Immediate Publication. Published on 06 Jan 2011 as manu

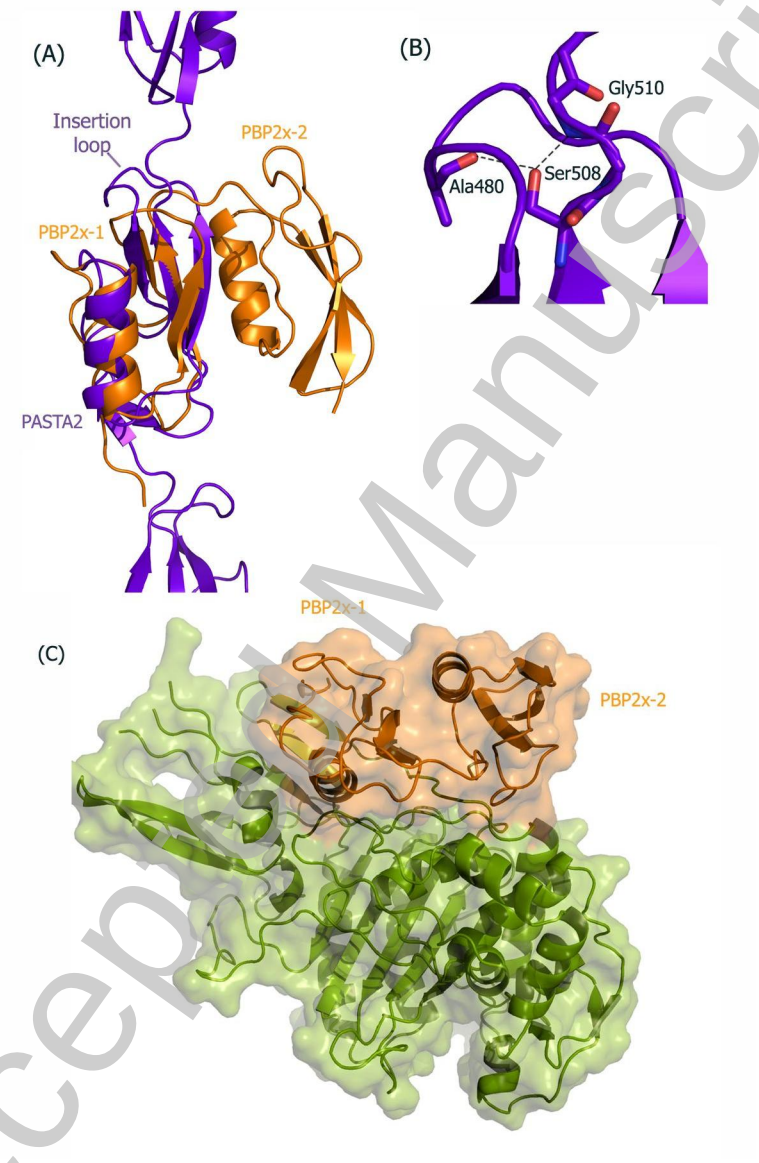

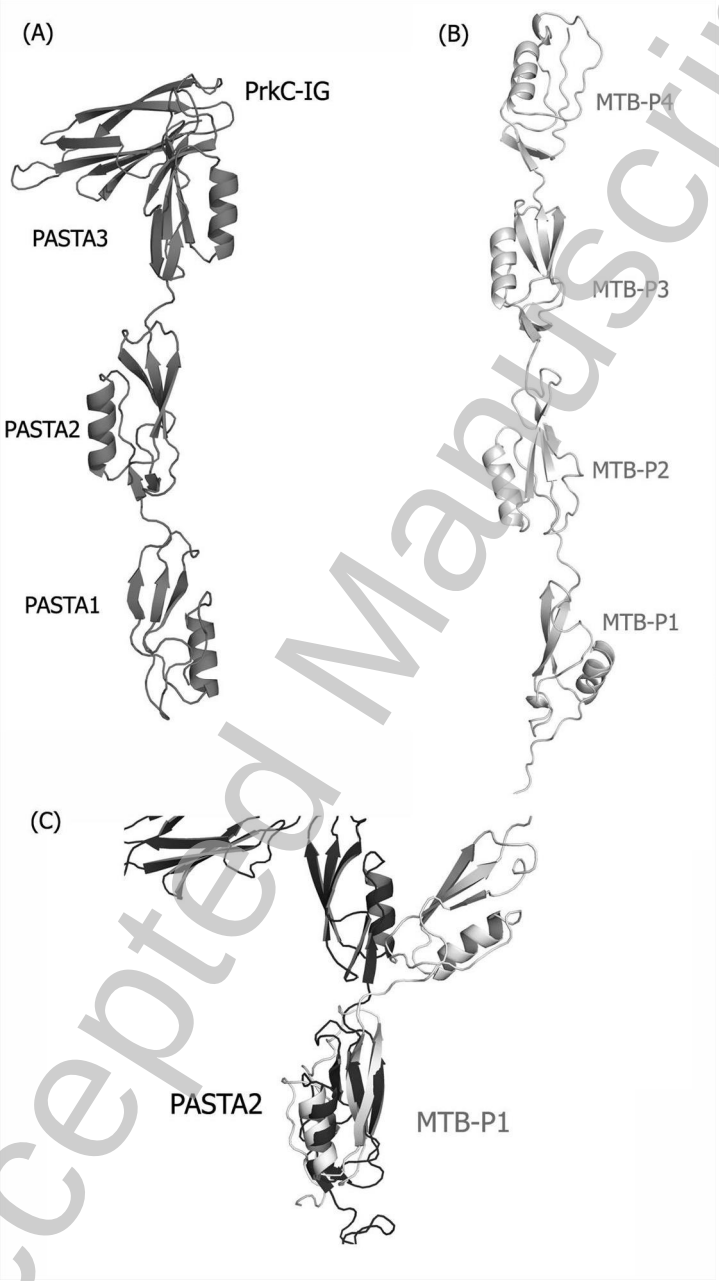

Biochemical Journal Immediate Publication. Published on 06 Jan 2011 as manuscript BJ20101